Targeted Delivery of Magnetic Cobalt Nanoparticles to the Eye Following Systemic Administration

Mirko Dengler[a], Katayoun Saatchi[a], James P. Dailey[b], Joanne Matsubara[c], Frederick S. Mikelberg[c], Urs O. Häfeli[a], Sonia N. Yeung[c]*

[a]*Faculty of Pharmaceutical Sciences, University of British Columbia, Vancouver, BC Canada*
[b]*Hamot Medical Center, Division of Ophthalmology, Erie, PA 16507, USA*
[c]*Department of Ophthalmology and Visual Sciences, Vancouver Hospital Eye Care Centre, University of British Columbia, Vancouver, BC, Canada*

* E-mail: sonia.y@gmail.com

Abstract. The eye offers a unique environment in the body to study progression and response to treatment of various ocular, vascular, and neurologic diseases as they occur in vivo. Due to its clear optical media, we can directly view blood vessels and nerve tissue, which often reflect the health of these tissues in the rest of the body. There are limitations to topical, periocular, or intraocular drug delivery that include access of the drug to the posterior segment of the eye and complications such as local scarring, hemorrhage, retinal detachment, cataract formation, or infection. The aim of this proof-of-concept study was to determine if systemically delivered magnetic cobalt nanoparticles (Co-MNP) could be directed to the eye of C57Bl mice via a unidirectional magnetic field. Both radioactive biodistribution studies and confocal imaging confirmed the increased presence of magnetic particles in the eye following magnetic targeting.

Keywords: Magnetic targeting, Drug delivery, Co-MNP, Ocular, Confocal microscopy
PACS: 87.85.Pq

INTRODUCTION

Nanocarriers, such as nanoparticles, have the capacity to deliver drugs to specified target sites. This technology, termed nanomedicine, is currently being investigated in several branches of ophthalmology for the therapy of many eye diseases [1-3]. Although the eye has the advantage of clear optical media for direct visualization of pathology, progression of disease, and response to treatment, it also has several drawbacks as a target organ for drug delivery [4]. The anterior segment of the eye is generally addressed with topical administration, while delivery to the posterior segment has largely been achieved through periocular and intraocular injection.

Direct administration to the posterior segment has inherent shortcomings such as repeated uncomfortable treatments to achieve constant therapeutic drug levels, bioavailability of the drug, local scarring and loss of delivery site access, infection, hemorrhage, and trauma to local tissues. Access to the posterior segment systemically is fraught with anatomic obstacles including the blood-retinal and blood-retinal pigment epithelial (RPE) barriers [5].

One way to overcome these obstacles is to target the eye with magnetic particles and hold or concentrate them at the target site with the help of a directed magnetic field. Initial experiments towards this aim were done by direct intraocular delivery of magnetically responsive elements such as very small steel balls [6] or nanosized magnetite particles made into a biocompatible ferrofluid [7]. But to our knowledge, no successful delivery of magnetic nanoparticles through the vascular system to the eye has been published. Here we report first results of the systemic delivery via tail vein injection of magnetic Co-MNP (Co-MNP) to the posterior segment of the eye in C57Bl mice following the application of a unidirectional magnetic field.

CP1311, *8th International Conference on the Scientific and Clinical Applications of Magnetic Carriers*
edited by U. Häfeli, W. Schütt, and M. Zborowski

EXPERIMENTAL DETAILS

Labeling of Magnetic Co-MNP (Co-MNP) with ^{99m}Tc

TurboBeads® (TurboBeads, Zurich, Switzerland) with amine functionality (> 0.1 mmol/g) were used for labeling with ^{99m}Tc [8]. An Isolink kit (Covidien, St. Louis), was used to prepare the tricarbonyl technetium [$^{99m}Tc(H_2O)_3(CO)_3^+$]. Before technetium labeling, a tridentate (N2O (2 + 1)) bifunctional ligand was bound to the surface of the particles using carbodiimide coupling. This formed a neutral metal complex with the $[Tc(CO)_3]^+$ core. [9]. Thermodynamic stability for *in vivo* applications of the particle-bound ^{99m}Tc was evaluated by a challenge study with the *in vivo* ligand cysteine [10]. For this purpose, the particles were incubated in a 0.1 M cysteine solution at 37 °C for 1 h and the bound radioactivity determined after magnetic separation in a gamma counter.

Cellular Toxicity Assay (MTT Assay)

The *in vitro* cytotoxicity of Co-MNP was tested using a modified cell viability assay [11]. The MTT assay is a colorimetric assay for which 5000 LCC6 breast cancer cells were plated, in 100 μL of media, into each well of a 96-well plate and incubated for 24 hours. These cancer cells served as sensitive indicators for toxicity. Fifty microliters of nanoparticles suspensions, $CoCl_2 \cdot 6H_2O$ solutions or supernatants/washes from nanoparticle suspensions at concentrations up to 5 mg/mL in media were added and incubated for 48 hours. The supernatant was carefully removed, and 100 μL of media and 20 μL of a 5 mg/mL MTT solution added and incubated for 3 more hours. Viable cells take up the MTT into their mitochondria and metabolize it into blue formazan crystals. As a control, 150 μL of PBS at pH 7.4 was added to cells in 8 of the wells. The supernatant in each well was aspirated and 150 μL of dimethyl sulfoxide (DMSO) added to solubilize the cells and MTT crystals. After 1 hour shaking on an Eppendorf Thermomixer at 37 ºC and 400 rpm to dissolve all crystals, the blue color was read in a multi-well scanning spectrophotometer at 540 nm. The cell viability was calculated by comparing the sample absorption to the one of the control cells, which was by definition 100%. Magnetic nanoparticles were considered toxic if the difference between cell growth inhibition of control and exposed cells was statistically significant at the 5% level, as determined by a t-test.

Animal Husbandry

Six-week-old C57Bl/6 mice were obtained from the breeding colony of the University of British Columbia (Vancouver, BC, Canada). All mice were fed ad libitum. All studies were in compliance with the ARVO Statement for the Use of Animals in Ophthalmic and Vision Research.

Systemic Delivery of Magnetic Nanoparticles

A summary of the experimental protocol is shown in Figure 1. C57Bl/6 mice were anesthetized with gas inhalational anesthesia (isoflurane and oxygen) and placed in a stereotactic frame. For magnetic targeting, a cylindrical magnet was placed in front of both eyes (Figure 2). Non magnet controls were positioned similarly without a magnet. Subsequently, 150 μL of ^{99m}Tc-labelled particles were injected into the tail veins of the mice with a 28 G insulin syringe. The particles were allowed to circulate for 30 minutes with or without the application of a unidirectional magnetic field before the mice were sacrificed.

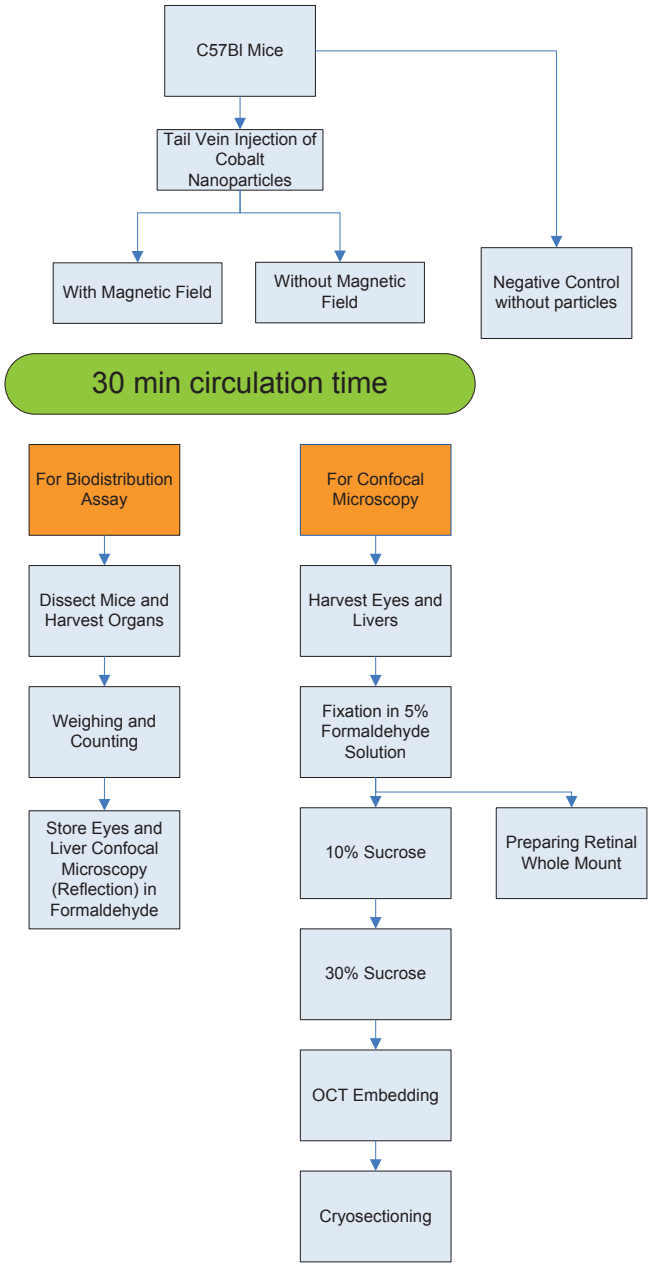

FIGURE 1. Block diagram of the overall experimental protocol.

Biodistribution Assay

Radioactivity was measured in the tail, blood, heart, liver, kidneys, lungs, small intestine, brain, muscle, bladder, spleen, stomach, left globe, right globe, and remaining body. The total and percentage of radioactivity per gram of tissue was measured for each sample.

Confocal Analysis of Co-MNP

Selected organs (left globe, right, globe, and liver) were removed for confocal analysis following tail vein injection of Co-MNP. Prior to fixation, the globes were perforated at the limbus with a 28 G needle to allow proper fixation of the retinal tissue. Organs were fixed in 5% formaldehyde in 0.1 M phosphate-buffered saline overnight at

4°C. Following fixation, the organs (globes and liver) were either embedded in O.C.T. medium (Tissue-Tek O.C.T.; Sakura Finetek, Zoeterwoude, The Netherlands) for sequential anterior-posterior cryosectioning (25-µm thick) or processed for retinal whole mounts (globes).

Retinal whole mounts were prepared by first removing the anterior segment of the eye following a sclerocorneal incision, and then carefully dissecting the retina from its attachment to the optic nerve. Two to four radial relaxing incisions were made. The retina was prepared as a flattened whole mount on a glass slide with 50% glycerol in PBS and a cover slip. Confocal laser scanning microscopy (Leica DM 2500 for Figs. 6B, C, E, F and Zeiss Meta 510 for Figs. 6A, D) was performed for reflectance to detect the nanoparticles.

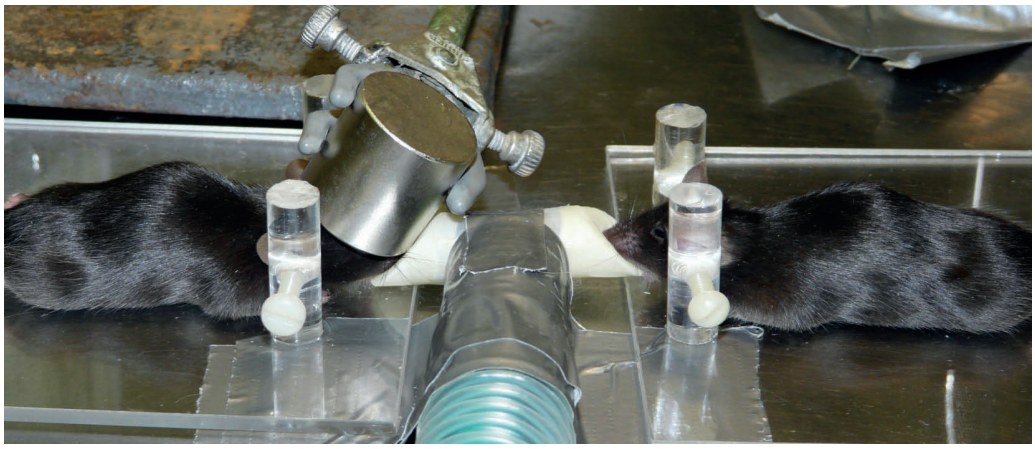

FIGURE 2. Photo depicting the experimental set-up of paired C57Bl mice with (left) and without (right) unidirectional magnetic targeting under inhalational anesthesia.

RESULTS AND DISCUSSION

Characterization of Co-MNP

The Co-MNP had a tendency to agglomerate, especially after magnetic separation. The reason for this became apparent upon taking a transmission electron picture of the samples (Figure 3A). The size distribution was much wider as expected, with a few of the particles approaching 100 nm in size. This size is far above the single domain size for cobalt, which also became apparent in the magnetization curve showing hysteresis (Figure 3B). Improvements are thus possible by narrowing the size distribution of the Co-MNP.

The derivatized Co-MNP were labeled with an average labeling efficiency of 52%. The radioactivity stayed particle-bound even during the cysteine challenge, with 90% of the ^{99m}Tc still on the particles after 1 h.

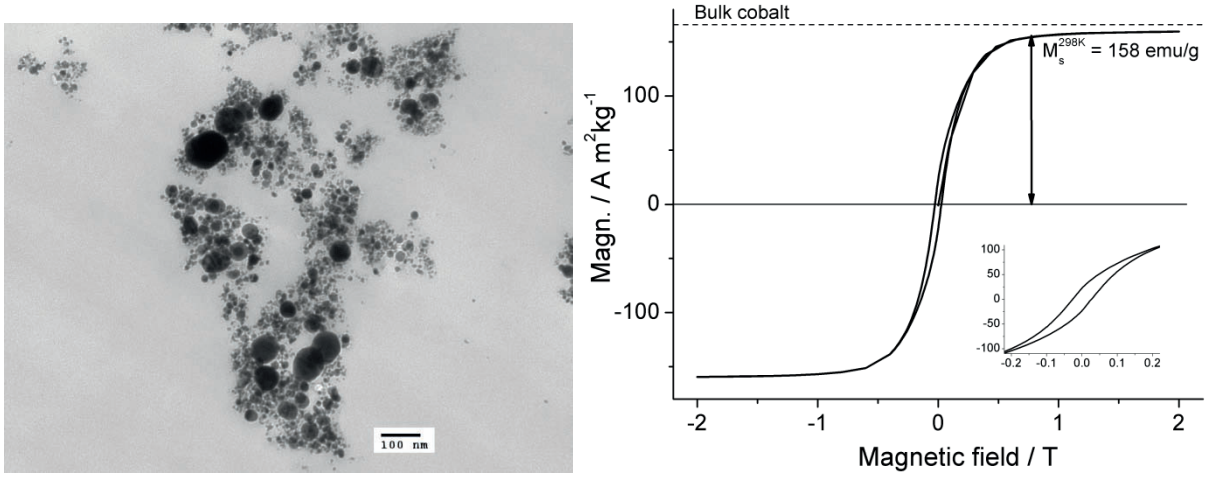

FIGURE 3. (A) Transmission electron microscopy of the Co-MNP used in this investigation. (B) The hysteresis in the magnetization curve confirms that some of the Co-MNP are ferromagnetic.

Freshly received Co-MNP showed a decrease in cell viability in the MTT assay already at 0.02 mg/mL (Figure 4). Since we did not expect such toxicity from tightly carbon-coated nanoparticles, as indicated by Grass *et al.*'s reported high oxidation resistance in air [8], we then washed the particles and checked both the washing liquid (supernatant) and the washed Co-MNP again for cell viability. While the wash liquid contained some removable toxic compound that resulted in a viability just below 60% (Figure 4), we saw no significant ($p<0.05$) cell toxicity below 2 mg/mL of Co-MNP any longer. Also, the supernatant of a second wash was 106.8± 6.8% and thereby not toxic. Using ICP-MS, we determined that there was less than 0.0001 mg/mL present as soluble cobalt in the second wash solution. It is thus advisable to wash freshly received magnetic particles not only for the purpose of having controlled conditions for ligand coupling, but also to remove potentially toxic ions released during storage. This is especially important for ions such as cobalt. We observed in a control experiment with $CoCl_2 \cdot 6H_2O$ that significant toxicities in the MTT assay were visible above 0.02 mg/mL of the salt (or 0.005 mg/mL of metallic cobalt).

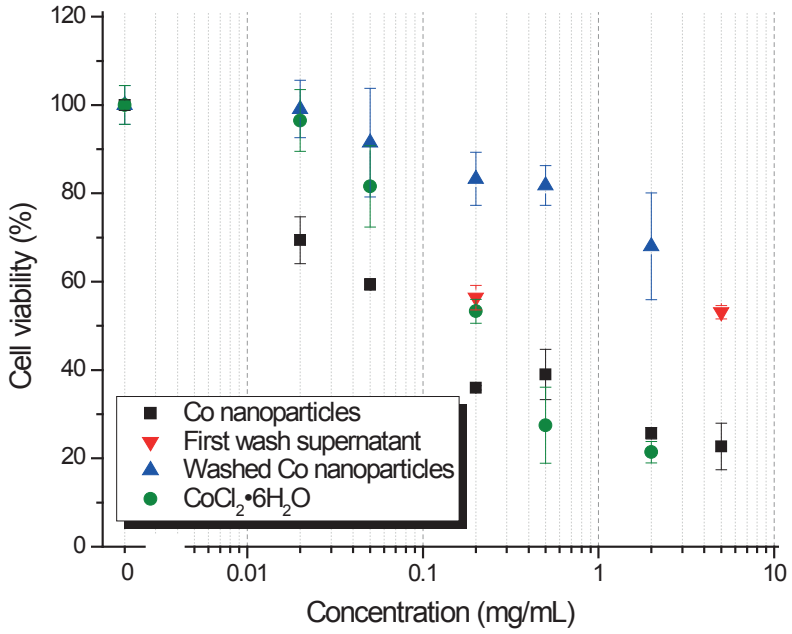

FIGURE 4. Cell viability testing of the magnetic Co-MNP.

Radioactive Biodistribution Assay

Following systemic administration of 3 mg of ^{99m}Tc-labeled Co-MNP and a 30 minute circulation time without magnetic targeting, radioactivity was found in all tested organs (Figure 5). Of note, the brain showed the lowest total activity after both eyes. As expected, the reticuloendothelial system consisting of the liver, lungs, and spleen showed high total activities and reflect the inherent properties of this system for filtering particles in the blood. These also represent particularly vascular tissue that may easily retain particles still in circulation at the time of sacrifice. The activity seen in the other organs may have been due to the presence of the particles in the small vessels within the tissue.

Figure 5 also shows a significant increase in total activity seen in both eyes and the brain following the application of a unidirectional magnetic field over a 30 minute circulation time. The magnet may have worked to draw and direct magnetic nanoparticles into local vessels more proximal to the magnetic field. It may also have acted to hold any magnetic nanoparticles that arrived at its proximity (brain and eyes) and thereby allowed the particles to enter into surrounding tissues. The exact mechanism by which the particles were able to get across the blood-retinal or blood-RPE barrier is still unknown. It is possible that they took advantage of molecular transport systems, were drawn directly into tissues by the strong magnetic field, or were endocytosed by local cells.

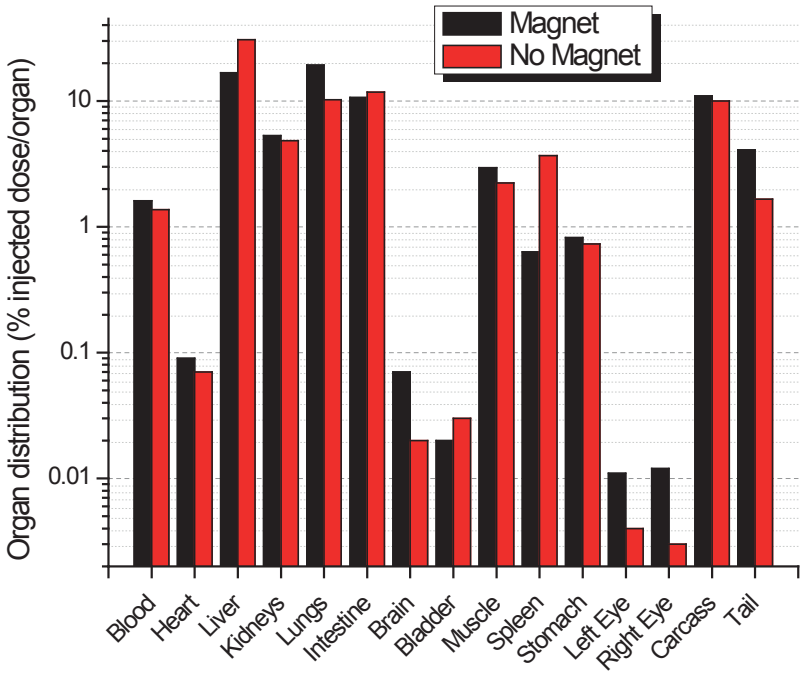

FIGURE 5. Logarithmic graphs of the total radioactivity found in various tissues following tail vein injection of magnetic Co-MNP with and without the application of a unidirectional magnetic field.

Confocal Laser Scanning Microscopy

Following systemic administration of 3 mg of Co-MNP and a 30 minute circulation time without magnetic targeting, no particles were detectable on reflectance mode in retinal whole mounts (Figures 6A) and anterior-posterior sections (Figure 6B). However, with magnetic targeting, many scattered nanoparticles were seen on reflectance mode in retinal whole mounts (Figure 6C) and anterior-posterior sections (Figure 6D). The color disparity between photos in Figure 6 is due to imaging by different confocal microscopes.

Figure 7A and 7B shows the presence of relatively more particles in liver sections without magnetic targeting when compared to liver sections following magnetic targeting. This may be due to fewer particles filtering through the liver with each circulation pass as a greater number of particles may be held in tissues more proximal to the magnet (brain and eyes).

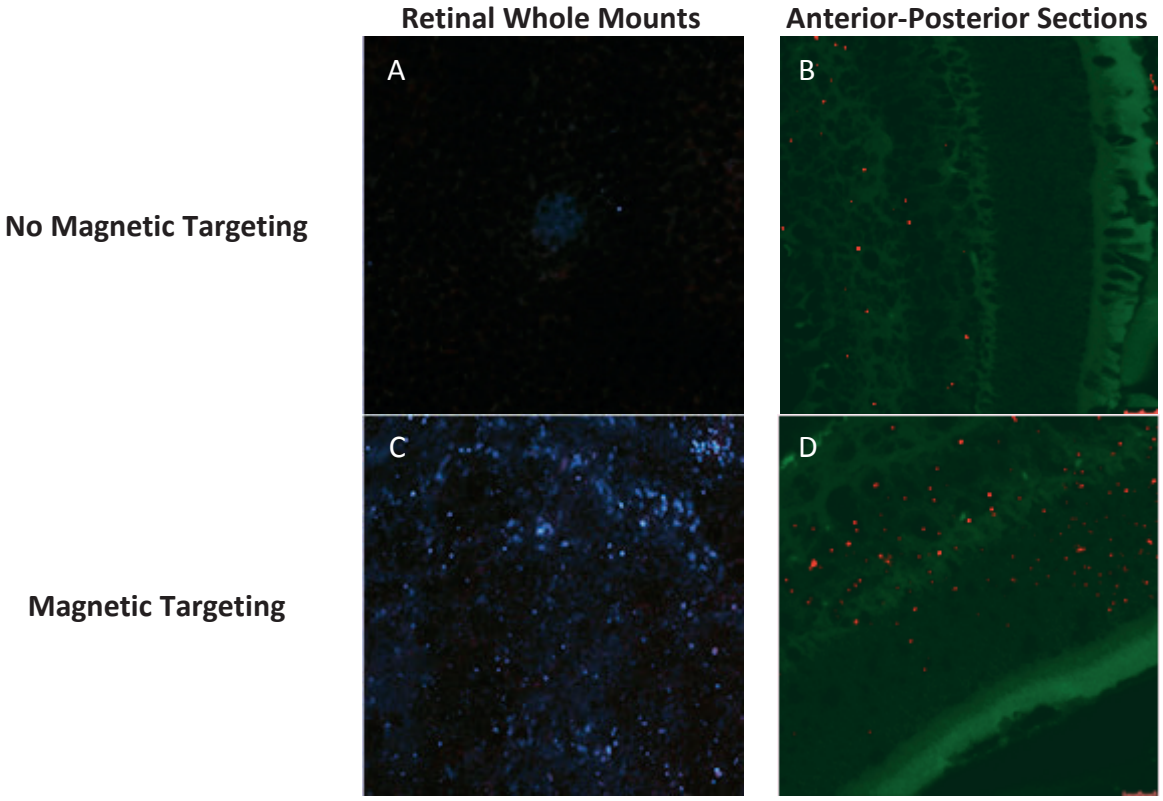

FIGURE 6. Confocal laser scanning images of magnetic Co-MNP in the retina on reflectance mode without (A-B) and with (C-D) the application of a unidirectional magnetic field. A and C are paired reflectance images of retinal whole mounts without and with magnetic targeting, respectively. Nanoparticles are seen as bright blue spots. C and D are paired reflectance images of anterior-posterior sections without and with magnetic targeting, respectively. Nanoparticles are seen as bright red spots. Differences in color between AC and BD are due to imaging by different confocal microscopes (see methods).

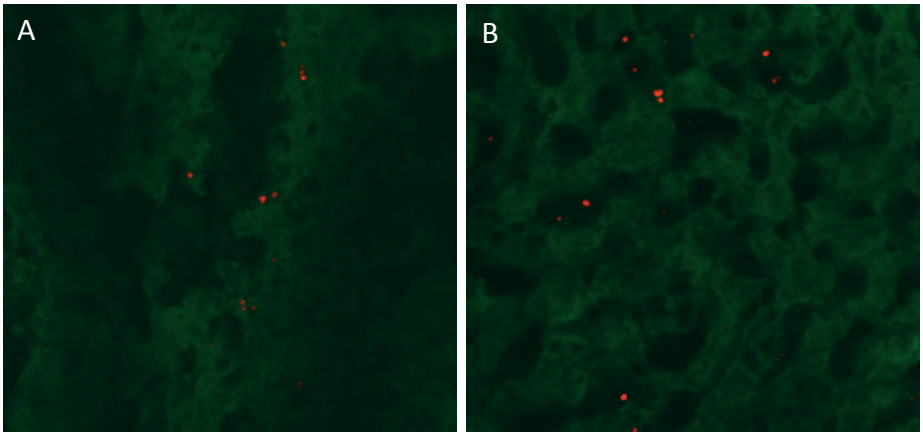

FIGURE 7. Confocal laser scanning images of magnetic Co-MNP in the liver on reflectance mode (A) with and (B) without the application of a unidirectional magnetic field.

The results of the confocal laser scanning imaging after systemic administration of magnetic Co-MNP with and without magnetic targeting confirm the results of the radioactive biodistribution studies. It is unclear whether the particles reside intra- or intercellularly, or whether some may remain within the retinal vessels. The pattern of reflectance suggests that at least some particles are likely within the retinal tissue itself and not completely held within the retinal vasculature. Further studies will be required to better localize these particles.

CONCLUSIONS

The systemic administration of targeted therapeutics such as magnetic nanoparticles for treatment of eye disease represents a new modality in ophthalmology. In these preliminary studies, we were able to show that systemically delivered magnetic nanoparticles can be targeted to ocular tissue following the application of a unidirectional magnetic field and detectable by both radioactive assay and confocal laser scanning microscopy. This could potentially avoid repeated local periocular or intraocular injections of medications and their associated risks. Despite the accumulation of the particles in the eye, their absolute concentration was very low, and they were found in all organs tested. We initially started out using the Co-MNP due to their known high magnetic response. However, our *in vitro* cellular toxicity assays showed that Co-MNP at higher concentrations affect cell viability and might thus also adversely affect the ocular tissues. In this regard, we are currently investigating the use of magnetite nanoparticles for systemic ocular targeting and delivery of therapeutics. Additional surface coatings might also help in further reducing potential toxicities.

There are challenges to this mode of delivery beyond the potential toxicity of the particles in the body. As the eye represents a small target organ with inherent protective barriers [2], it is difficult to achieve high levels of particles in this location in sufficient amount to treat ophthalmic diseases. To increase the amount of particles that may reach and enter ocular tissues, different particles sizes and concentrations, magnetic field strengths and constructs, and surface coating modifications will need to be examined. Furthermore, gene delivery may be another avenue that would increase the efficiency of achieving a therapeutic quantity of disease-modifying agents [12].

Despite these challenges, preliminary proof-of-principle experiments have demonstrated that this new method of delivery is feasible and may be an alternative or adjunct to conventional local treatments. Further investigation will be required to improve the efficiency of delivery, and to determine where the particles are accumulating in the eye and whether this may be modifiable for cell-specific targeting.

ACKNOWLEDGMENTS

The authors would like to thank Pfizer Canada and Nanomedics LLC for unrestricted research grants that supported this work.

REFERENCES

1. Y. Diebold and M. Calonge, *Prog. Retin. Eye Res.* in press (2010).
2. S. Wadhwa, R. Paliwal, S. R. Paliwal, et al., *Curr. Pharm. Des.* **15**, 2724 (2009).
3. R. Gaudana, J. Jwala, S. H. Boddu, et al., *Pharm. Res.* **26**, 1197 (2009).
4. X. Cai, S. Conley, and M. Naash, *Vision Res.* **48**, 319 (2008).
5. J. Barar, A. R. Javadzadeh, and Y. Omidi, *Expert Opin Drug Deliv* **5**, 567 (2008).
6. D. Lobel, J. R. Hale, and D. B. Montgomery, *Am. J. Ophthalmol.* **85**, 699 (1978).
7. D. L. Holligan, G. T. Gillies, and J. P. Dailey, *Nanotechnology* **14**, 661 (2003).
8. R. N. Grass, E. K. Athanassiou, and W. J. Stark, *Angew. Chem. Int. Ed. Engl.* **46**, 4909 (2007).
9. K. Saatchi and U. O. Häfeli, *Bioconjug. Chem.* **20**, 1209 (2009).
10. D. J. Hnatowich, F. Virzi, M. Fogarasi, et al., *Nuclear medicine and biology* **21**, 1035 (1994).
11. R. Pieters, D. R. Huismans, A. Leyva, et al., *Br. J. Cancer* **59**, 217 (1989).
12. S. Conley and M. Naash, *Prog. Retin. Eye Res.* **29**, 376 (2010).